ADVANCED FUNCTIONAL MATERIALS

DOI: 10.1002/adfm.200600278

Self-Organized Gradient Hole Injection to Improve the Performance of Polymer Electroluminescent Devices

By *Tae-Woo Lee*,* *Youngsu Chung*, *Ohyun Kwon*, and *Jong-Jin Park*

A new approach to forming a gradient hole-injection layer in polymer light-emitting diodes (PLEDs) is demonstrated. Single spin-coating of hole-injecting conducting polymer compositions with a perfluorinated ionomer results in a work function gradient through the layer formed by self-organization, which leads to remarkably efficient single-layer PLEDs (ca. 21 cd A^{-1}). The device lifetime is significantly improved (ca. 50 times) compared with the conventional hole-injection layer, poly(3,4-ethylenedioxythiophene)/poly(styrene sulfonate). These results are a good example for demonstrating that the shorter lifetime of PLEDs compared with small-molecule-based organic LEDs (SM-OLEDs) is not mainly due to the inherent degradation of the polymeric emitter itself. Hence, the results open the way to further improvements of PLEDs for real applications to large-area, high-resolution, and full-color flexible displays.

1. Introduction

The development of organic devices has been driven by a growing demand for low-cost and flexible electronic devices and information displays. Polymer light-emitting diodes (PLEDs) using solution processes can be promising candidates for large-area, high-resolution, fast-response, and full-color flexible displays. Although a great deal of progress has been made in improving the luminous efficiency and lifetime of solution-processed PLEDs since their discovery in 1990,[1] the reliability of PLED devices is still much behind that of vacuum-deposited small-molecule-based organic light-emitting diodes and still does not meet the requirements for commercialization toward full-color emissive displays.[2] Interface engineering between the anode and the emitting layer is important for the improvement of the device lifetime as well as luminous efficiency in PLEDs. Previous literature reports described several approaches to interface engineering that resulted in improving the device performances of organic light-emitting diodes, for instance, i) anode modification by plasma treatment,[3,4] ii) chemical modification of the anode,[5–7] iii) introducing a hole-injection layer (HIL),[8–17] and iv) a hole-transporting interlayer between the HIL and emitting layer.[18–20] Hole-injecting conducting polymer films such as polyaniline, polypyrrole, and poly(3,4-ethylenedioxythiophene) (PEDOT)[10–13] on indium tin oxide (ITO) play important roles to improve the device efficiency and the stability, because they can improve the hole injection from the ITO (work function: ca. 4.7–5.0 eV) and planarize the ITO surface. PEDOT/poly(styrene sulfonate) (PSS) compositions in aqueous solution are commercially available as the well-known Baytron P series HIL materials from H. C. Starck GmbH.[21] However, PEDOT/PSS has a relatively low work function of ca. 5.0–5.2 eV[21] so that the hole injection could be a limiting factor in the device performance in cases where the overlying layer has a much lower highest occupied molecular orbital (HOMO) level with respect to the vacuum level. For example, since the HOMO level of poly(9,9-dioctylfluorene) has been estimated to be –5.9 eV,[22] the hole-injecting energy barrier between PEDOT/PSS and poly(9,9-dioctylfluorene) can be as large as 0.7–0.9 eV. To overcome such a large hole-injection barrier between ITO and the HOMO of the emitting layer, a hole-injection layer with gradually increasing work function from the ITO side toward the emitting layer could be the most appropriate solution. Here, we achieved the fabrication of such HIL with gradient work function by self-organization.

Although the device lifetime can be greatly improved by introducing a PEDOT/PSS layer, the acidic nature of PEDOT/PSS etches ITO and as such indium can migrate into the PEDOT/PSS layer.[23] In addition, recent investigations on failure mode of PLEDs suggested that the polymeric HIL itself can be one of the dominant failure causes.[24] Therefore, at this stage of PLED development, it is much required to modify the HIL to further improve the device lifetime as well as efficiency. In this work, we show that single spin-coating of a conducting polymer composition with a perfluorinated ionomer (PFI) forms a hole-injection layer with a gradient work function by self-organization of the PFI, which resulted in a remarkably improved device lifetime and efficiency. We formulated a hole-injecting conducting polymer composed of commercially available PEDOT/PSS for OLED applications and a PFI. Since the fluorocarbon chains in the PFI are more hydrophobic than polystyrene sulfonate, the PFI tends to preferentially self-organize at the surface of the film. Our investigations by UV photoelectron spectroscopy and molecular orbital calculations showed that higher concentrations of PFI resulted in higher work functions, and X-ray photoelectron spectroscopy (XPS) and time-of-flight secondary ion mass spectroscopy (TOF-SIMS) measurements confirmed that PFI tends to reside

---

[*] Dr. T.-W. Lee, Dr. Y. Chung, Dr. O. Kwon, Dr. J.-J. Park
Samsung Advanced Institute of Technology
Mt. 14–1, Nongseo-dong, Giheung-gu, Yongin-si
Gyeonggi-do 449–712 (Korea)
E-mail: taew.lee@samsung.com

mainly at the upper part of the film. Therefore, the HIL film can have a gradient work function according to the concentration gradient of PFI in the film, which resulted in remarkable improvement in luminous efficiency of the device. We also found that the newly formulated HIL with PFI significantly blocks the migration of In and Sn into the emitting layer, which implies that the HIL layer can act as an appropriate buffer layer for improving the device lifetime.

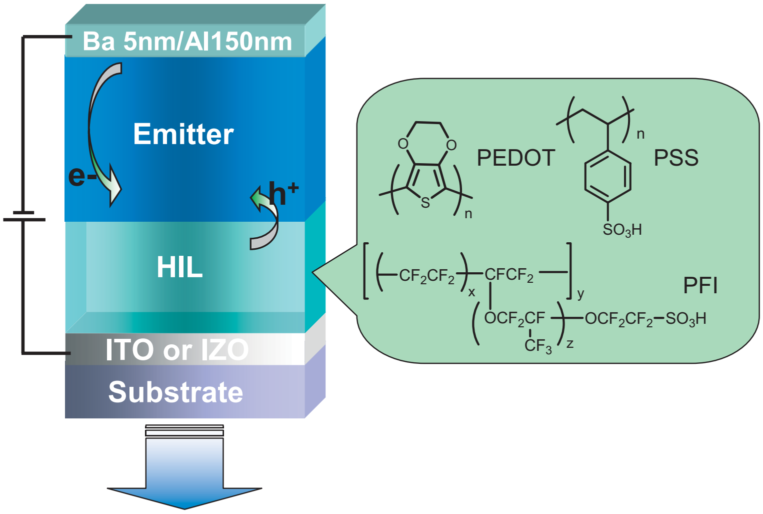

Figure 1. The PLED device structure and the chemical structures of the components of conducting polymer compositions used for HILs.

Table 1. The work-function levels of five different conducting polymer compositions.

Sample code	PEDOT/PSS/PFI	Work function (AC2) [eV]
AI4083	1:6:0	5.20
AIPF161	1:6:1.6	5.55
AIPF81	1:6:3.2	5.63
AIPF41	1:6:6.3	5.72
AIPF21	1:6:12.7	5.79
AIPF11	1:6:25.4	5.95

Table 2. Calculated dipole moments, ionization potential (IP), and deprotonation energy (DP) of the end groups obtained by density-functional theory calculations. Debye (D) ≈ 3.33564×10^{-30} C m; 1 kcal = 4.184 kJ; Ph: phenyl.

Compounds	IP [eV]	DP [kcal mol^{-1}]	Dipole moment (neutral) [D]	Dipole moment (DP) [D]
$CH_3CH_2SO_3H$	–8.287	336.3	3.395	4.935
$CF_3CF_2SO_3H$	–9.316	316.0	2.800	6.248
$CH_3CH_2CH_2SO_3H$	–8.265	336.1	3.505	6.835
$CF_3CF_2CF_2SO_3H$	–9.171	315.0	2.669	8.914
CH_3–O–CH_2SO_3H	–7.910	333.7	4.596	7.159
CF_3–O–CF_2SO_3H	–9.342	315.5	2.741	7.967
CH_3CH_2–O–CH_2SO_3H	–7.814	334.0	4.502	8.908
CF_3CF_2–O–CF_2SO_3H	–9.348	314.6	2.704	10.280
CH_3–O–$CH_2CH_2SO_3H$	–7.424	332.8	2.681	8.154
CF_3–O–$CF_2CF_2SO_3H$	–9.248	314.4	2.578	10.107
$(CH_3)_2CH$–O–CH_2–$(CH_3)CH$–O–$CH_2CH_2SO_3H$	–6.943	332.6	3.807	19.522
$(CF_3)_2CF$–O–CF_2–$(CF_3)CF$–O–$CF_2CF_2SO_3H$	–9.264	314.3	2.719	21.940
Ph–SO_3H	–7.549	332.5	4.361	8.116
CH_3–Ph–SO_3H	–7.273	333.6	4.900	10.226
CF_3–Ph–SO_3H	–7.988	325.4	2.390	11.477
CH_3CH_2–Ph–SO_3H	–7.221	333.8	4.973	12.152
CF_3CF_2–Ph–SO_3H	–8.000	324.9	2.526	14.596
$(CH_3)_2CH$–Ph–SO_3H	–7.252	333.3	3.950	13.310

2. Results and Discussion

Figure 1 shows the chemical structures of the materials we used to formulate our conducting polymer compositions for the HIL in OLEDs. A 5 wt % perfluorosulfonate ionomer in a mixture of water and alcohol (4.5:5.5, v/v), was purified via dialysis using a molecular porous membrane (cut-off molecular weight: 2000). Commercially available PEDOT/PSS for OLED applications (Baytron P VP AI4083) at a 1:6 weight ratio in aqueous solution was used, because of its low conductivity (6×10^{-4} S cm^{-1}). We reformulated the commercial PEDOT/PSS compound by adding 5 wt % PFI resin. The work-function levels according to the compositions were measured by ultraviolet photoelectron spectroscopy in air (surface analyzer, model AC2, Riken Keiki, Co., Ltd., Japan). The results are summarized in Table 1. This table shows that the work-function levels increase as the content of PFI increases. Eventually, we obtained a composition with a very high work function (ca. 5.55–5.95 eV). To understand the effect of PFI on the electronic properties of the compositions, density-functional theory (DFT)[25] calculations were applied to obtain the ionization potential (IP), the deprotonation energy (DP), and the dipole moments of various end groups as shown in Table 2. All calculations were performed at the B3LYP/6–31G(d,p) level by using the Gaussian 98 program.[26] We compared fluorocarbon sulfonic acids with hydrocarbon (alkyl and alkyl-substituted benzene (Ph)) sulfonic acids with changing chain lengths. The calculated IP level of a fluorocarbon sulfonic acid is lower than that of corresponding hydrocarbon sulfonic acids (i.e., $CF_3CF_2SO_3H$ versus $CH_3CH_2SO_3H$). Because of the electron-withdrawing ability of fluorine atoms it is more difficult to oxidize a fluorocarbon sulfonic acid than its corresponding hydrocarbon one. It should be noted that the calculated IP level becomes higher (i.e., closer to the vacuum level) as the hydrocarbon alkyl chain length increases but the IP level does not change when the fluorinated alkyl chain length becomes longer. This implies that the fluorinated alkyl sulfonic acid in a polymeric form (i.e., PFI) still has a lower IP level compared to the corresponding pure alkyl sulfonic acid. When an ether group (–O–) is inserted into the chain, the IP level becomes higher for hydrocarbon sulfonic acids (i.e., $CH_3–O–CH_2SO_3H$ versus $CH_3CH_2SO_3H$) but lower for fluorocarbon sulfonic acids (i.e., $CF_3–O–CF_2SO_3H$ versus $CF_3CF_2SO_3H$). When a phenyl group is inserted between the alkyl group and the SO_3H unit, the IP level becomes higher for both hydrocarbon and fluorocarbon sulfonic acids. These findings suggest that polymers with fluorocarbon sulfonic acids such as PFI can also have lower IP levels with respect to the vacuum level than polystyrene sulfonic acids. PFI molecules can be more easily deprotonated than PSS. Calculated dipole moments indicate that the increase of dipole moment ($\Delta\mu$) between the neutral form and the deprotonated form are larger for fluorocarbon sulfonic acids than corresponding hydrocarbon ones, which leads to the fact that when PFI molecules chemically react with the ITO surface after deprotonation, the holes can be more easily induced by the large dipole moments near the ITO surface. To observe the effect of PFI on the work function of the ITO surface, we formed a self-assembled monolayer on the ITO surface by immersing the UV-ozone-treated ITO into a 0.5 wt % PFI solution. Then, it was observed that the water contact angle of the PFI-modified ITO was increased from 55° to 81° which implies that the surface became highly hydrophobic and the work function was also increased by ca. 0.5 eV. Judging from all the information above, the high work-function energy levels in the PEDOT/PSS/PFI compositions most probably stem from the properties of the PFI itself.

We used XPS to find out the surface composition and molecular distribution versus depth. Figure 2 shows the S 2p spectrum of the film spincast from a commercial PEDOT/PSS aqueous solution. The spectrum can be deconvoluted in four doublet peaks at 164.5, 166.6, 168.4, and 168.9 eV. We used the energy difference of 1.2 eV between S $2p_{1/2}$ and $2p_{3/2}$ with a fixed area ratio of 0.5. The doublet peaks at about 169 eV can be assigned to the sulfonic acids in the PSS. The components at 168.4 and 168.9 eV correspond to the PSS^- salt and PSSH, respectively.[27] The peak at 164.5 eV has been assigned to the sulfur atoms in PEDOT.[27] Besides these, a very small peak at about 166.6 eV was added for satisfactory fitting. This peak can be assigned to an intermediate state, sulfone (–SO_2–) between atomic-like sulfur (PEDOT) and SO_3^-.

Figure 3 shows the molecular depth profiles using deconvoluted S 2p peaks for PEDOT, sulfonic acid, sulfone and sulfide. We used the sum of the peak areas of PSSH and PSS^- salt to calculate the concentration of sulfonic acid. The sulfide component at about 162 eV increased near the interface with ITO. This may result from the reaction between sulfur and ITO by Ar^+ sputtering during depth profiling. For mixtures of PEDOT/PSS with PFI, we used the C 1s peak at 292 eV to calculate the PFI concentration. This peak can be assigned to CF_2, evidently resulting from PFI.

As shown in Figure 3, PSS is a main surface component for conventional PEDOT/PSS and its concentration drops abruptly and shows even bulk distributions up to a sputter time of 22 min. Due to the increase of the sulfide component, the PSS concentration decreases slightly after 22 min, whereas PFI is rich at the surface for the mixtures with PFI and its concentration gradually decreases with depth. We also confirmed that the surfaces of mixtures with PFI were covered with fluorinated carbon using TOF-SIMS as shown in Figure 4.

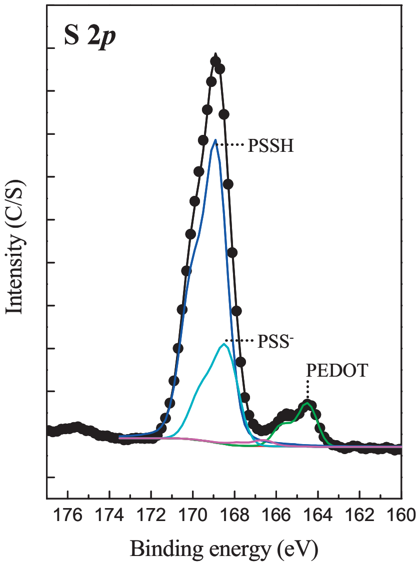

Figure 2. S 2p core-level spectrum of conventional PEDOT/PSS (Baytron P VP AI4083).

Figure 4 shows the positive mass spectra of samples obtained using TOF-SIMS. The spectra for Baytron P VP AI4083 mainly show the hydrocarbon peak series from the polystyrene of PSS. We can also see that the spectra for the mixtures of PEDOT/PSS with PFI are very similar, regardless of the PFI content. They show intense peaks for the $C_nF_m^+$ fragments,

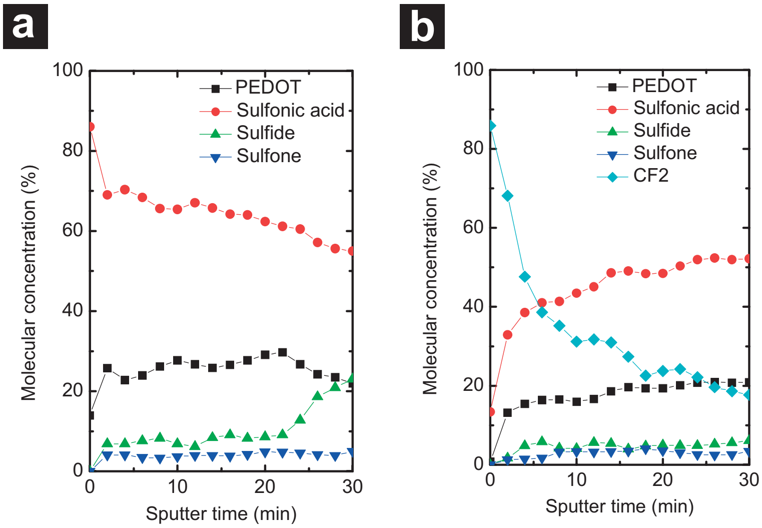

Figure 3. Molecular depth profiles for the HILs of a) conventional PEDOT/PSS and b) the newly formulated PEDOT/PSS/PFI (AIPF41). Deconvoluted S 2p peaks for PEDOT, sulfonic acid, sulfide, and sulfone concentrations and C 1s peak at 292 eV for the PFI concentration were used.

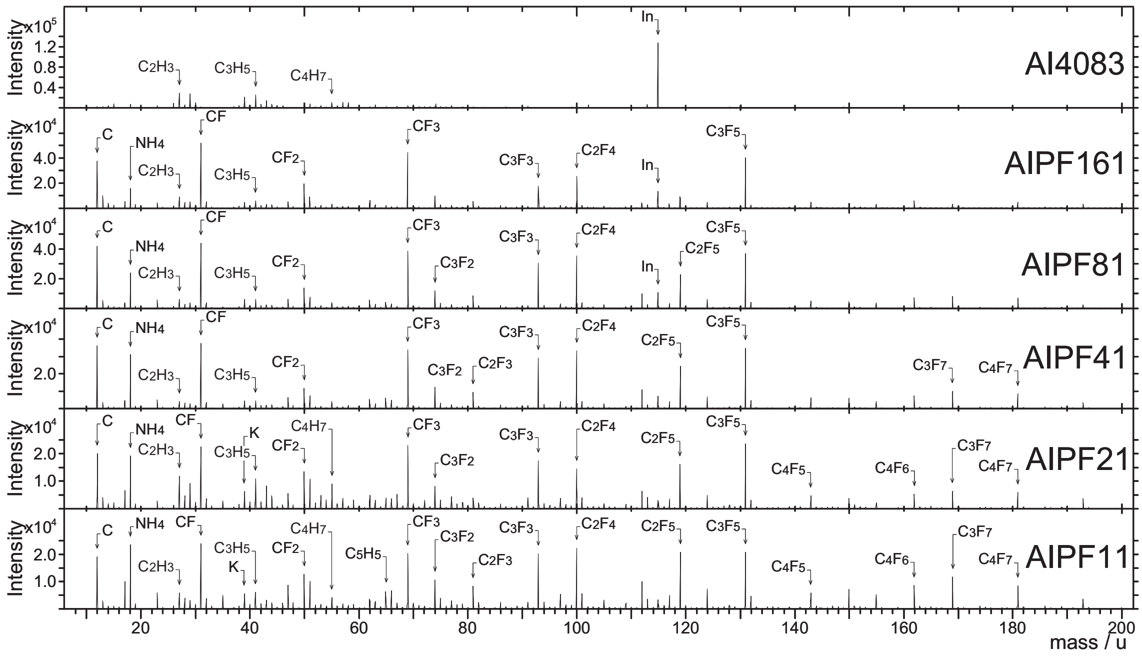

Figure 4. The positive mass spectra of time-of-flight secondary ion mass spectroscopy data for the HILs.

which are characteristics of fluorinated polymers. It clearly indicates the surfaces are mostly covered with PFI, even in small concentrations of PFI, which is consistent with the XPS data as shown in Figure 3.

The gradual increase of PFI toward the top surface could make the work function increase from the bottom to the top surface. Figure 5 illustrates the schematic energy diagram of the PLED devices to compare the self-organized gradient HIL (Fig. 5b) with conventional PEDOT/PSS (Fig. 5a). As shown in Figure 5b, the work function of the HIL gradually increases and thus the hole can be efficiently injected into the emitting layer despite of the large energy barrier between ITO and the HOMO level of the emitting layer. We tested the current density of two different hole-only devices (anode: IZO, cathode: Au) using a PEDOT/PSS/PFI layer or a PEDOT/PSS layer. The device using the PEDOT/PSS/PFI layer showed a much higher hole current density than the device using the PEDOT/PSS layer, which implies that the PEDOT/PSS/PFI layer improves hole injection in PLED devices. Figure 6 shows the plots of ^{115}In and ^{120}Sn peaks for the HIL surfaces on ITO measured by TOF-SIMS. The intensities of the In (Fig. 6a) and Sn (Fig. 6b) peaks greatly decreased when adding more PFI. This indicates that the fluorinated surface of this new HIL can greatly reduce the diffusion of In and Sn from the ITO anode into the emitting layer and therefore act as a diffusion buffer against ITO, which is possibly an important role to improve the device lifetime.

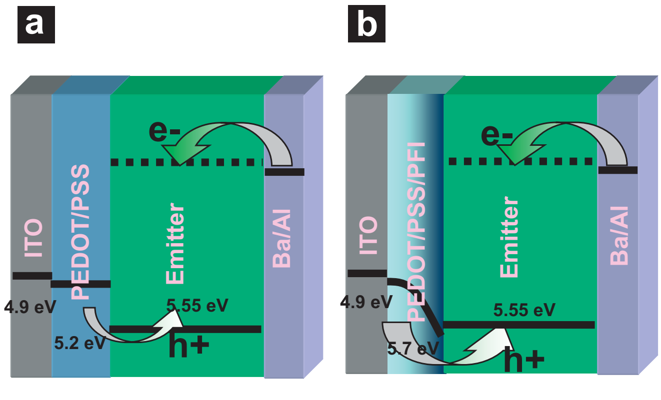

Figure 5. Schematic energy diagram of the devices using a) conventional PEDOT/PSS and b) PEDOT/PSS/PFI compositions as the HIL.

We fabricated green-light-emitting polyfluorene PLEDs by using our conducting polymer compositions (PEDOT/PSS/PFI) as a HIL and compared our results with devices using a conventional PEDOT/PSS HIL. When we fabricated the device using our PEDOT/PSS/PFI compositions on ITO (4.9 eV), the maximum luminous efficiency we obtained was 15.1 cd A^{-1} which is much higher than that (10.0 cd A^{-1}) of the device with PEDOT/PSS. The best device efficiency (ca. 21 cd A^{-1}) was found in devices using an indium zinc oxide (IZO) anode (5.1 eV) instead of ITO due to the more favorable hole injection from the IZO to the bottom side (> 5.1 eV) of the PEDOT/PSS/PFI layer. The maximum efficiency (9.8 cd A^{-1}) of a device with PEDOT/PSS on IZO was similar to that (10.0 cd A^{-1}) of the device with PEDOT/PSS on ITO because the hole-injection barrier from PEDOT/PSS into the emitting layer is still high (ca. 0.35 eV). Therefore, as Figure 7a shows, we compared the device luminous efficiencies for a device using the PEDOT/PSS/PFI composition on IZO with a device using conventional PEDOT/PSS on IZO. The device with PEDOT/PSS/PFI on IZO showed much higher efficiency values (15.2 times higher at 100 cd m^{-2}, 6.3 times higher at

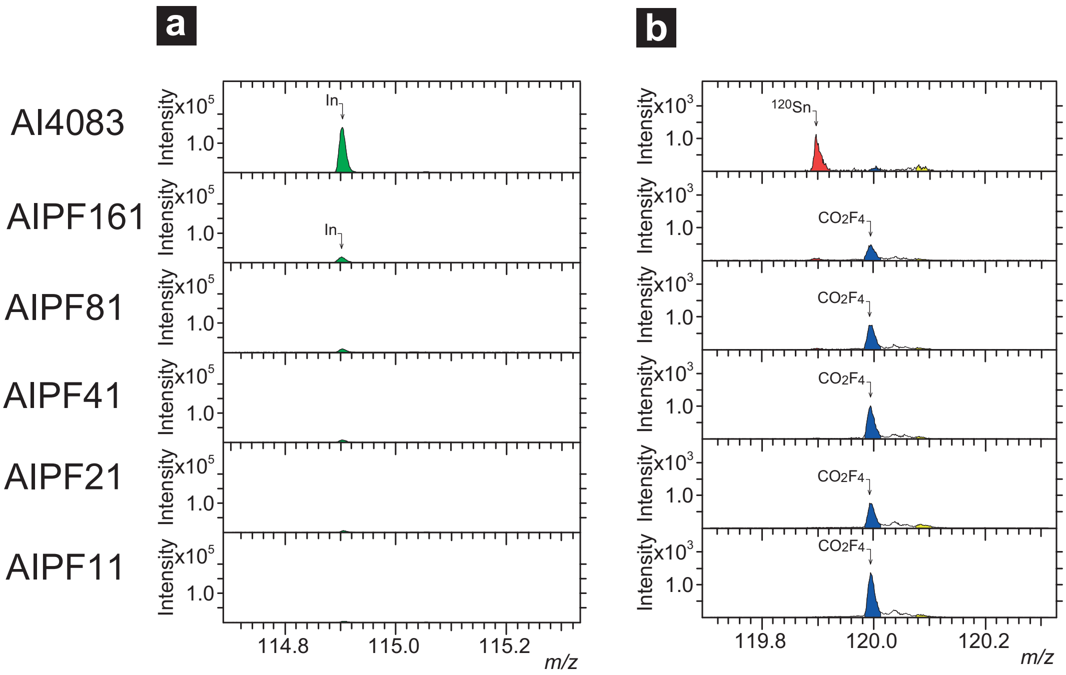

Figure 6. High resolution mass spectra at a) $m/z = 115$ and b) $m/z = 200$ for 6 conducting polymers with different compositions.

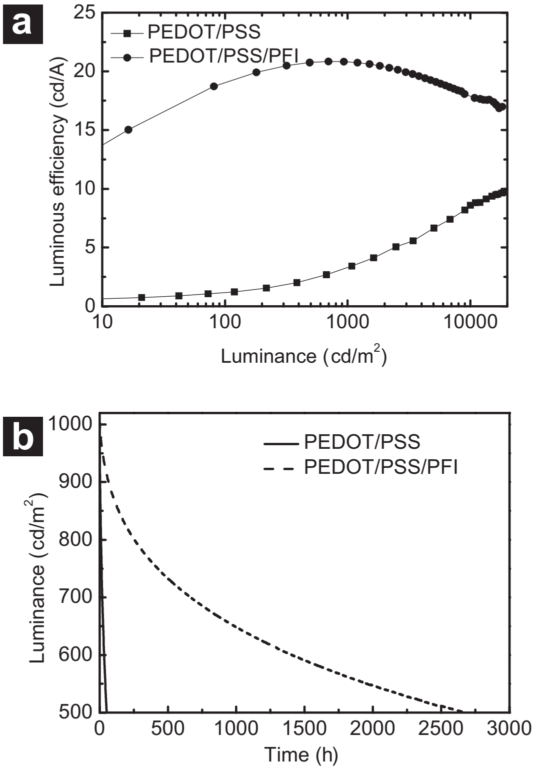

Figure 7. Device luminous efficiency and device lifetime. a) The luminous efficiency versus luminance for devices using PEDOT/PSS (■) and PEDOT/PSS/PFI (AIPF41) (●) as the HIL in the structure of IZO/HIL/green emitter/Ba/Al. b) The device lifetime with initial luminance 1000 cd m^{-2} for the devices using PEDOT/PSS and PEDOT/PSS/PFI as a HIL.

1000 cd m^{-2}) in function of the luminance than those of the device with PEDOT/PSS on IZO, which resulted from the efficient hole injection from the IZO to the emitter via the PEDOT/PSS/PFI layer and more balanced electron–hole recombination.

We also tested the device lifetime of the device using PEDOT/PSS/PFI at initial luminance 1000 cd m^{-2} after 5 min aging at 1000 cd m^{-2} as shown in Figure 7b. The half-lifetime (2680 h at 1000 cd m^{-2}) of the device using PEDOT/PSS/PFI was dramatically improved compared with the half-lifetime (52 h at 1000 cd m^{-2}) of the device using PEDOT/PSS. The maximum luminous efficiency and the half-life of the device using the PEDOT/PSS layer that are obtained after the emitting polymer film was baked at 130 °C for 15 min are reasonable values according to the previous literature for devices using green-light-emitting polyfluorene derivatives.[28,29] Therefore, the remarkable improvement indicates that the compositions including perfluorinated ionomers can be one of the promising hole-injection buffer materials for enhancing the device lifetime. Since the fluorocarbon sulfonic acids in the HIL preferentially reside on the film surface, this type of HIL can effectively block the impurities stemming from PEDOT/PSS and ITO (alkali metal, sulfate, In, Sn, etc.). The fluorocarbon has intrinsically a good chemical stability and hydrophobicity. In fact, our HIL materials are less sensitive to moisture relative to conventional PEDOT/PSS. In this respect, the greatly improved lifetime can be ascribed to the effective diffusion-barrier characteristics of the PFI as well as the improved electron–hole balance for recombination by gradient hole injection resulting in a lower driving current density at the same luminance. We are still trying to further improve the lifetime by optimizing the film annealing temperature and the device characteristics, such as electrode structure and thickness, and by using purified PEDOT/PSS and PEDOT/PSS/PFI.[30]

3. Conclusion

We demonstrated an approach to interface engineering to form gradient hole injection via the single spin-coating of conducting polymer compositions with PFI by self-organization, which improves the device efficiency and lifetime significantly. The gradient in the hole-injection layer was proven by photoelectron spectroscopy (AC2 and XPS) and TOF-SIMS analysis. The luminous efficiency we achieved was as high as ca. 21 cd A^{-1}, which could be attributed to nearly balanced charge injection leading to near-perfect recombination. Although conventional PEDOT/PSS exhibited relatively low work-function levels of ca. 5.0–5.2 eV, our PEDOT/PSS/PFI compositions showed very high work-function levels (ca. 5.55–5.95 eV). The concentration of PFI in the composition tends to gradually increase from the ITO toward the emitting layer, which leads to efficient hole injection. The PFI can effectively block the In and Sn migration from the ITO into the emitting layer. The improved electron–hole balance for recombination and the diffusion barrier characteristics of the PFI lead to a remarkably improved device lifetime. The significantly improved performance of PLEDs using this new HIL implies that the PLED performance can be further improved for real commercialization by using development approaches in devices other than the molecular design of the reliable emitting material. The controllability of the work function of these conducting polymer compositions and the barrier properties can be widely used for charge-injecting contact to improve the device performance in other various organic electronic and optoelectronic devices.

4. Experimental

4.1. Computational Details

Density-functional theory (DFT) calculations were applied to fluorocarbon sulfonic acids (PFI end groups) and hydrocarbon sulfonic acids (PSS end groups) in order to compare ionization potentials and deprotonation energies as shown in Table 2. The first ionization potential was calculated as the difference between the energy of the neutral molecule and the energy of the radical cationic state based on the neutral geometry. The deprotonation energy is calculated from the energy difference between the deprotonated form (X-) and the protonated from (XH). Geometries of the protonated forms (neutral) and deprotonated forms (radical anion) were fully optimized at the B3LYP/6–31G(d,p) level by using the Gaussian 98 program. Calculated dipole moments of the protonated and deprotonated forms were also calculated at the same level of theory.

4.2. X-ray Photoelectron Spectroscopy (XPS)

The X-ray photoelectron spectroscopy (XPS) measurements were carried out using a PHI Q2000 system equipped with a monochromatized Al Kα source. The binding energies were calibrated to the C 1s peak at 285.0 eV. Depth profiling with XPS was conducted to obtain the molecular profiles. We used low energy Ar^+ at 500 eV to minimize sputtering-induced damage. However, we found out that even when using 500 eV, the concentration of sulfonic acids was underestimated by the transformation of sulfonic acids to other states such as atomic sulfur or sulfides. Using a reference sample which was composed of only PSS, we corrected the PSS concentration.

4.3. Time-of-Flight Secondary Ion Mass Spectroscopy (TOF-SIMS)

Time-of-flight secondary ion mass spectroscopy measurements were performed using an ION-TOF IV. The high-mass resolution spectrum for each sample surface was acquired using a 25 keV Bi^+ ion source. The examined area was 200 μm × 200 μm for each sample.

4.4. PLED Fabrication and Characterization

The hole-injection layers (HILs) (PEDOT/PSS or PEDOT/PSS/PFI compositions) were spin-coated to give 60 nm films on top of indium-tin-oxide (ITO: work function 4.9 eV) or indium-zinc-oxide (IZO: work function 5.1 eV)/glass in air and then immediately baked on the hotplate in a N_2 glove box at 200 °C for 10 min. A green-light-emitting polyfluorene derivative (LUMATION 1300 series Green Polymer, Dow Chemical Company (currently Sumitomo), $M_n = 190\,000$, $M_w = 350\,000$, HOMO: –5.55 eV, LUMO: –3.05 eV) dissolved in toluene was spin-coated on the HIL layers to obtain a thickness of 80 nm, and was subsequently baked at 100 °C for 15 min. The 5 nm Ba and 150 nm Al layers were sequentially deposited on the emitting layer under vacuum below 5×10^{-7} Torr. The PLED devices were encapsulated with a glass lid by using a UV-curable epoxy resin. The current–voltage–luminescence (*I–V–L*) characteristics were obtained with a Keithley 238 source measure unit and a Photo Research PR650 spectrophotometer. The device lifetime was recorded by using a McScience Polaronix OLED Lifetime Test System.

Received: March 28, 2006
Revised: June 30, 2006

---

[1] J. H. Burroughes, D. D. C. Bradley, A. R. Brown, R. N. Marks, K. Mackay, R. H. Friend, P. L. Burns, A. B. Holmes, *Nature* **1990**, *347*, 539.
[2] H. K. Chung, presented at IMID'2005, Seoul, Korea, July 2005.
[3] J. S. Kim, R. H. Friend, F. Cacialli, *Appl. Phys. Lett.* **1999**, *74*, 3084.
[4] J. X. Tang, Y. Q. Li, L. R. Zheng, L. S. Hung, *J. Appl. Phys.* **2004**, *95*, 4397.
[5] B. Choi, J. Rhee, H. H. Lee, *Appl. Phys. Lett.* **2001**, *79*, 2109.
[6] S. Kato, *J. Am. Chem. Soc.* **2005**, *127*, 11 538.
[7] Q. Huang, G. Evmenenko, P. Dutta, P. Lee, N. R. Armstrong, T. J. Marks, *J. Am. Chem. Soc.* **2005**, *127*, 10 227.
[8] S. Kim, C. Hsu, C. Zhang, H. Skulason, F. Uckert, D. LeCoulux, Y. Cao, I. Parker, *J. Inf. Disp.* **2004**, *5*, 14.
[9] T.-W. Lee, O. Kwon, M.-G. Kim, S. H. Park, J. Chung, S. Y. Kim, Y. Chung, J.-Y. Park, E. Han, D. H. Huh, J.-J. Park, L. Pu, *Appl. Phys. Lett.* **2005**, *87*, 231 106.
[10] Y. Yang, E. Westerweele, C. Zhang, P. Smith, A. J. Heeger, *J. Appl. Phys.* **1995**, *77*, 694.
[11] R. W. T. Higgins, N. A. Zaidi, A. P. Monkman, *Adv. Funct. Mater.* **2001**, *11*, 407.
[12] S. A. Carter, M. Angelopoulos, S. Karg, P. J. Brock, J. C. Scott, *Appl. Phys. Lett.* **1997**, *70*, 2067.
[13] J. Gao, A. J. Heeger, J. Y. Lee, C. Y. Kim, *Synth. Met.* **1996**, *82*, 221.
[14] M. Gross, D. C. Müller, H.-G. Nothofer, U. Scherf, D. Neher, C. Bräuchle, K. Meerholz, *Nature* **2000**, *405*, 661.

[15] P. K. H. Ho, J.-S. Kim, J. H. Burroughes, H. Becker, S. F. Y. Li, T. M. Brown, F. Cacialli, R. H. Friend, *Nature* **2000**, *404*, 481.

[16] A. Elschner, F. Bruder, H.-W. Heuer, F. Jonas, A. Karbach, S. Kirchmeyer, S. Thurm, R. Wehrmann, *Synth. Met.* **2000**, *111–112*, 139.

[17] a) X. Zhang, A. S. Shetty, S. A. Jenekhe, *Macromolecules* **1999**, *32*, 7422. b) X. Zhang, S. A. Jenekhe, *Macromolecules* **2000**, *33*, 2069.

[18] T.-W. Lee, M.-G.. Kim, S. Y. Kim, S. H. Park, O. Kwon, T. Noh, T.-S. Oh, *Appl. Phys. Lett.* **2006**, *89*, 123 505.

[19] J.-S. Kim, R. H. Friend, I. Grizzi, J. H. Burroughes, *Appl. Phys. Lett.* **2005**, *87*, 023 506.

[20] H. Yan, P. Lee, N. R. Armstrong, A. Graham, G. A. Evmenenko, P. Dutta, T. J. Marks, *J. Am. Chem. Soc.* **2005**, *127*, 3172.

[21] The material information is available from the H. C. Starck website, http://www.hcstarck.com (accessed December 2006).

[22] S. Janietz, D. D. C. Bradley, M. Grell, C. Giebeler, M. Inbasekaran, E. P. Woo, *Appl. Phys. Lett.* **1998**, *73*, 2453.

[23] M. P. de Jong, L. J. van IJendoorn, M. J. A. de Voigt, *Appl. Phys. Lett.* **2000**, *77*, 2255.

[24] X. Crispin, S. Marciniak, W. Osikowicz, G. Zotti, A. W. Denier van der Gon, F. Louwet, M. Fahlman, L. Groenendaal, F. de Schryver, W. R. Salaneck, *J. Polym. Sci. B: Polym. Phys.* **2003**, *41*, 2561.

[25] W. Koch, M. C. Holthausen, *A Chemist's Guide to Density Functional Theory*, Wiley & Sons, New York **2000**.

[26] *Gaussian 98, Revision A.9*, M. J. Frisch, G. W. Trucks, H. B. Schlegel, G. E. Scuseria, M. A. Robb, J. R. Cheeseman, V. G. Zakrzewski, J. A. Montgomery, Jr., R. E. Stratmann, J. C. Burant, S. Dapprich, J. M. Millam, A. D. Daniels, K. N. Kudin, M. C. Strain, O. Farkas, J. Tomasi, V. Barone, M. Cossi, R. Cammi, B. Mennucci, C. Pomelli, C. Adamo, S. Clifford, J. Ochterski, G. A. Petersson, P. Y. Ayala, Q. Cui, K. Morokuma, D. K. Malick, A. D. Rabuck, K. Raghavachari, J. B. Foresman, J. Cioslowski, J. V. Ortiz, A. G. Baboul, B. B. Stefanov, G. Liu, A. Liashenko, P. Piskorz, I. Komaromi, R. Gomperts, R. L. Martin, D. J. Fox, T. Keith, M. A. Al-Laham, C. Y. Peng, A. Nanayakkara, C. Gonzalez, M. Challacombe, P. M. W. Gill, B. G. Johnson, W. Chen, M. W. Wong, J. L. Andres, M. Head-Gordon, E. S. Replogle, J. A. Pople, Gaussian, Inc., Pittsburgh PA, **1998**.

[27] G. Greczynski, T. Kugler, W. R. Salaneck, *Thin Solid Films* **1999**, *354*, 129.

[28] J. Kim, J. Lee, C. W. Han, N. Y. Lee, I.-J. Chung, *Appl. Phys. Lett.* **2003**, *82*, 4238.

[29] M. C. Suh, H. K. Chung, S.-Y. Kim, J. H. Kwon, B. D. Chin, *Chem. Phys. Lett.* **2005**, *413*, 205.

[30] The device efficiency was quite reproducible irrespective of the purification of the HIL material when the devices were fabricated at the same conditions, but the device lifetime was improved by further purification of the HIL material. The lifetime data we show here is not the best we have obtained up to now.